# Computational studies of the stability of the $(H_2O)_{100}$ nanodrop


Annika Lenz and Lars Ojamäe





Original Publication:

Annika Lenz and Lars Ojamäe, Computational studies of the stability of the $(H_2O)_{100}$ nanodrop, 2010, Journal of Molecular Structure: THEOCHEM, (944), 1-3, 163-167.
http://dx.doi.org/10.1016/j.theochem.2009.12.033

# Computational studies of the stability of the $(H_2O)_{100}$ nanodrop

Annika Lenz and Lars Ojamäe

Department of Chemistry, IFM, Linköping University, SE-58183 Linköping, Sweden

---

**Abstract**

The stability of the $(H_2O)_{100}$ nanodrop, experimentally known from a polyoxomolybdate crystal structure (Müller et al. *Inorg. Chem. Commun*., 2003, 6, 52) and other structures inferred from clathrate structures and from the literature, are studied by quantum-chemical B3LYP and MP2 computations. Positions for the H atoms in the 100-molecule cluster are suggested, which will then be of $C_{2h}/C_i$-symmetry when considering the oxygens/all atoms. The free energies are compared to the trends for smaller clusters with 15-30 molecules. For the small clusters both cage-based structures and denser structures with a larger number of H-bonds obtained from Bandow and Hartke who used an evolutionary algorithm (Bandow and Hartke, *J. Phys. Chem. A*, 2006, 110, 5809) are investigated. The dense structures are most often found to be lower in electronic energy. The cage-based structures, to which the structure of the experimentally found $(H_2O)_{100}$ cluster can be categorized, gain in stability when their Gibbs free energies at 298 K are considered, although which of a dense or a cage-based structure that is predicted to be the most stable depends on the quantum-chemical method employed. Additional cage-based clusters in the 35-81 molecular range were constructed for comparison. The constructed $(H_2O)_{42}$ cluster has an extraordinary high symmetry ($S_6$), even when the hydrogens are considered. The experimental cluster with 100 molecules and the constructed cluster with 42 molecules are found to be in fair agreement with a plausible overall global minimum energy vs. cluster size trend inferred from the smaller clusters.

Keywords:

1. **water clusters**
2. **quantum-chemical computations**
3. **hydrogen bonding**
4. **B3LYP calculations**
5. **Gibbs free energy**

## 1. Introduction

A $(H_2O)_{100}$ nanodrop of water has been experimentally identified in the cavity of a polyoxomolybdate crystal structure by Müller et al [1]. The crystallographic data gives the oxygen framework, which shows a symmetric ($C_{2h}$) cluster based on the dodecahedral 20-mer cage surrounded by 60 water molecules in 5-membered rings (Fig. 1). The 5-membered rings are connected to the central dodecahedron by 20 molecules, which each H-bonds to three of the rings and to the dodecahedron. For the nanodrop situated in the crystal the outer molecules H-bond to the surrounding atoms of the polyoxomolybdate crystal, which causes all water molecules to be 4-coordinated. Can the structure of this $(H_2O)_{100}$ cluster also be considered as a possible structure for a gas phase cluster?

There are two main ideas concerning the structures of low energy structures of water clusters [2-4]. Cage-based clusters, like the low energy structures for the clusters with 21 and 28 molecules [5-8], consist of a 3-coordinated cage that may enclose a number of molecules H-bonded to the surrounding cage. Quantum-chemical calculations most often predict more dense structures [2,3]. Also the global-minimum structures as predicted using the TTM2-F potential often are fairly dense structures where the molecules have high coordination numbers [9]. For small and medium sized cluster a larger number of 4-coordinated molecules implies that more H-bonded rings with 4 members must be formed. In the experimentally known structures (dodecahedral clusters [10,11], $(H_2O)_{100}$ nanodrop[1], clathrates [12], ice) 4-membered rings are rare. The strain in 4-membered rings will be higher than in 5- or 6-membered rings since the O-O-O angle is significantly smaller than the tetrahedral H-O-H angle in the water molecule. The structure for the $(H_2O)_{100}$ cluster is a cage-based cluster with the outer 60 molecules 3-coordinated and without any 4-membered rings. In this study, the stability of the $(H_2O)_{100}$ nanodrop with the experimentally found oxygen framework [1] is compared with smaller clusters. For the small cluster the relative stability between cage-based and the more dense TTM2-F global energy-minimum conformations was investigated. Quantum-chemical B3LYP computations are performed to derive geometry-optimized structures, energies and thermodynamic corrections though harmonic vibrational analysis.

## 2. Method and Results

Electronic energies and Gibbs free energies are obtained from quantum-chemical computations. The geometries of all clusters were optimized using the B3LYP [13,14] hybrid density functional and the 6-31+G(d,p) [15] basis set. This method gives a mean O-O distance (2.76 Å) for the dodecahedral $(H_2O)_{20}$ cluster which is near 2.78 Å, the distance obtained with the 6-311++G(2df,2pd) basis set [2]. Gibbs free energies (from vibrational harmonic normal-mode computations) are calculated at 298 K using B3LYP. Single-point MP2 energies were calculated for the optimized B3LYP geometries. The calculations were performed using the

GAUSSIAN03-program [16]. The energies are presented as interaction energies per water molecule: $\Delta E = E(\text{cluster}) / n(\text{H}_2\text{O}) - E(\text{monomer})$. Interaction energies and Gibbs free energies for the optimized clusters are given in Tables 1 and 2.

Structures for cage-based clusters with 15-22, 28 and 30 molecules were taken from Refs [4,7,17-20] (Fig. 2). More dense structures containing 15-34 molecules were obtained from Bandow and Hartke [9], who derived the structures using an evolutionary algorithm where the TTM2-F potential was used to model the intermolecular interactions (Fig. 3). Coordination and energy results for the optimized clusters are listed in Table 1. The reoptimization of the TTM2-F structures in some cases resulted in clusters with 5-coordinated molecules.

For the 100-molecule cluster the oxygen framework was taken from the experimental crystal structure [1]. In addition structures for clusters with 35, 42, 54, 55, 80 and 81 molecules were constructed where the outer oxygen frameworks were based on the cage structures found in clathrates [21] and fullerene structures [22], and that were allowed to contain a small number of water molecules in the interior of the cluster. For all clusters hydrogens were added to the oxygen framework: to ensure that low-energy H-bonded networks were obtained, the hydrogens were positioned guided by the energy-structure rules derived from studies of smaller clusters [4,17-19,23]. For the 100-molecule cluster the symmetry thereby was decreased from $C_{2h}$ to $C_i$. The so obtained structure for the 100-molecule cluster is shown in Fig. 1 and the structures for the clusters with 35, 42, 54, 55, 80 and 81 molecules are shown in Fig. 4.

In a structure-H clathrate [21] the largest cage is formed by 36 water molecules which are arranged in 12 pentagons and 8 hexagons ($5^{12}6^{8}$). Starting from this cage and by placing six molecules in the interior, a high symmetric 42 cluster can be formed (Fig. 4 and Table 2). It is noteworthy that the high symmetry ($S_6$) can be preserved also when the hydrogens are considered. A smaller cluster with 35 molecules similar to the cluster with 42 molecules based on 5-instead of 6-membered rings was also constructed.

Larger cages were built by utilizing the $C_{48}$ ($5^{12}6^{14}$) and $C_{60}$ ($5^{12}6^{20}$) fullerene structures [22] for the oxygen framework. When a 6-membered ring is placed inside the cage with 48 molecules a 54 cluster is formed, and by adding an extra molecule inside a 55-mer is obtained. 80-/81-mer clusters are constructed by including a 20-/21-mer in the 60-membered cage. Coordinations, symmetries and energies are listed in Table 2.

### 3. Discussion

The electronic interaction energies obtained using B3LYP and MP2 are shown in Fig. 5 and Table 1. The interaction energy per molecule decreases irregularly with increasing cluster size but at a slower rate as the clusters grow larger, see Fig. 5. If one assumes that the cluster energy is directly proportional both to the number of molecules at the surface and to the number in the interior of the cluster, it follows that the energy should approximately follow an $n^{-1/3}$ behavior. Curves with the formulas $\Delta E_{B3LYP} = -54.5 + 13.4(n - 11.1)^{-1/3}$ and $\Delta E_{MP2} = -65.4 + 34.6(n - 5.6)^{-1/3}$ can be fitted to the computed energies. As the cluster grows the energy functions asymptotically approach -54.5 kJ mol$^{-1}$ (B3LYP) and -65.4 kJ mol$^{-1}$ (MP2), or -49 kJ mol$^{-1}$ (B3LYP) and -55 kJ mol$^{-1}$ (MP2) if the energies are scaled so that for the water dimer the computed and the experimental (-11.3 kJ mol$^{-1}$ [24]) interaction energies coincide:

$$\Delta E(\text{scaled}) = \Delta E(\text{calc}) \frac{\Delta E(\text{dimer, exp})}{\Delta E(\text{dimer, calc})}. \qquad (1)$$

The MP2 scaled large-size energy limit of -55 kJ mol$^{-1}$ lies in between estimated values for the lattice energy of ice, -53.0 kJ mol$^{-1}$ [25] and -58.8 kJ mol$^{-1}$ [26]. Besides a difference in magnitude between the interaction energies obtained from MP2 vis-à-vis B3LYP, the energy vs. cluster size trends from the two methods are seen in Fig. 5 to be similar, especially for the larger clusters. One can also notice that the energy of the cluster with 21 molecules, the same number of molecules that causes an enhanced peak in experimental mass spectra for charged clusters [8,27,28], has an energy that lies on the fitted energy curves.

In Fig. 5 it is seen that there is a significant spread around the fitted energy function for the dense TTM2-F global minimum structures [9] using the reoptimized B3LYP energies. But if instead the MP2 energies are used (i.e. single-point MP2 calculations for the B3LYP-reoptimzed TTM2-F structures) the energies closely follows the fitted curve. The TTM2-F structures are also generally lower in energy than the cage-based structures of the same sizes, and this trend is more pronounced when MP2 is used instead of B3LYP. This is an indication that the TTM2-F potential manages to supply relative water interaction energies and minimum structures in agreement with those one can obtain from (much lengthier) MP2 calculations. That TTM2-F and MP2 results for water clusters can be in good agreement has also been found previously [3].

The energies of the clusters with 42 and 100 molecules are close to energies predicted from the energy curves fitted to the global minimum structures of the smaller clusters. For the B3LYP computations they even lie lower than the curve, but considering the worse fit of the energy function for the small clusters to the B3LYP energies than to the MP2 energies, and

considering that MP2 is generally considered superior to B3LYP, the extrapolation using the fitted MP2 energy curve is probably more realistic. (The MP2 energy of the 100-molecule cluster is slightly above the value predicted from the curve, but this is very dependant on which functional form is used for the curve.) Since the energy function was fitted to probable global energy minimum structures, the positioning of the 100- and 42-molecule cluster energies close to the fitted energy curve shows that it can not be ruled out that these structures do correspond to global energy minima for these particular sizes, although it admittedly does not constitute a proof.

The electronic energy differences between the cage-based clusters and the denser structures with 15-21, 28 and 30 molecules are shown in the top part of Fig. 6. The more dense TTM2-F global minimum structures (reoptimized using B3LYP) that contain a higher fraction of H-bonds per molecule are generally more stable than the cage structures when $\Delta E$ is considered (which confirms the success of the energy-minima search algorithm and potential choice in Ref. [9]). The Gibbs free energies at 298 K were calculated using B3LYP. Since the free energies were obtained using the harmonic frequencies, these energies are only approximate, but probably still accurate enough to let us infer some general trends. No calculation of free energies was carried out using MP2. Instead the free energy corrections obtained from the B3LYP calculations were simply added to the MP2 interaction energies. The free energy corrections are seen in Fig. 6 to decrease the energy differences between the cage-based and the denser clusters. Using B3LYP, the cage-based structures even become more stable than the denser structures when free energies are considered, but the situation is most often still the opposite if MP2 is used. (There are other phenomena that will also influence the relative free energies, such as different entropies due to different H-bond topologies [29]: for example, for one mol of the cluster with 20 molecules the H-bond configurational entropy is 125 J/K for the cage-based or dodecahedral cluster and 102 J/K for the dense cluster, as obtained using the coordination data in Table 1 and formula B1 in Ref. [29].)

In Fig. 7 the Gibbs free energy is displayed for the different cluster sizes. The free energy per water molecule diminishes with increasing cluster size (causing the $(H_2O)_{100}$ nanodrop to be the lowest in free energy of the clusters studied), although any systematic Gibbs free energy vs. cluster size relation such as that for the interaction energy in Fig. 5 is not evident in Fig. 7. For example the 21 cluster is lower in free energy than the adjacent cluster sizes. Possibly also the 42 cluster appears to be quite low in free energy, but for this cluster and for the 100 cluster data on the adjacent cluster sizes are lacking. $\Delta G$ at 298 K is positive by several kJ for all clusters studied, why only minute amounts would be present under standard conditions

## 4. Conclusions

Approximate expressions for the electronic interaction energy per molecule of global-minimum water clusters as a function of cluster size was derived, where the energy limit for large clusters is close to the experimental energy of ice. The expressions were obtained by fitting to B3LYP and MP2 energies of cage-based and more dense [9] clusters with up to 34 molecules. The denser clusters are generally lower in electronic energy than the cage-based structures. Gibbs free energy corrections diminish the energy difference between the cage-based and denser structures. The $(H_2O)_{100}$ nanodrop of $C_i$ symmetry with the oxygen framework taken from experiments [1] and a constructed $(H_2O)_{42}$ cluster, which has a very high symmetry ($S_6$) even when the hydrogens are considered, are found to possess energies that are in fair agreement with the energies obtained from the fitted global-minimum energy vs. cluster size expressions.

## 5. Acknowledgements

This research is supported by the Swedish Research Council (VR) and the Swedish supercomputer centers SNAC.

*Electronic supplementary information (ESI) available*: Data files in Xmol format containing the structural coordinates for the clusters in Figs. 1 and 4.

## 6. References

[1] A. Müller, H. Bögge, E. Diemann, Inorg. Chem. Commun., 6 (2003) 52.

[2] A. Lenz, L. Ojamäe, Chem. Phys. Lett., 418 (2006) 785.

[3] G. S. Fanourgakis, E. Apra, S. S. Xantheas, J. Chem. Phys., 121 (2004) 2655.

[4] A. Lenz, L. Ojamäe, J. Phys. Chem. A, 110 (2006) 13388.

[5] U. Nagashima, H. Shinohara, N. Nishi, H. Tanaka, J. Chem. Phys., 84 (1986) 209.

[6] C.-C. Wu, C.-K. Lin, H.-C. Chang, J.-C. Jiang, J.-L. Kuo, M. L. Klein, J. Chem. Phys., 122 (2005) 074315.

[7] A. Kahn, J. Chem. Phys., 99 (1995) 12450.

[8] J. Q. Searcy, J.B. Fenn, J. Chem. Phys., 61 (1974) 5282.

[9] B. Bandow, B. Hartke, J. Phys. Chem. A, 110 (2006) 5809.

[10] J.L. Kassner, Jr, D.E. Hagen, J. Chem. Phys., 64 (1976) 1860.

[11] S. Wei, Z. Shi, A. W. Castleman, Jr., J. Chem. Phys., 94 (1991) 3268.

[12] E. D. Sloan, Clathrate hydrates of natural gases, (Dekker, New York 1990 ) Electronic reproduction. Boca Raton, Fla.: CRC Press, 2008.

[13] A. D. Becke, Phys. Rev. A, 38 (1998) 3098.

[14] C. Lee, W. Yang, R.G. Parr. Phys. Rev. B, 37 (1988) 785.

[15] W. J. Hehre, R. Dichfield, J. A. Pople, J. Chem. Phys., 56 (1972) 2257.

[16] M.J. Frisch, et al., Gaussian 03, Gaussian Inc., Wallingford CT, 2004.

[17] A. Lenz, L. Ojamäe, Phys. Chem. Chem. Phys., 7 (2005) 1905.

[18] D. J. Anick, J. Mol. Struct. (THEOCHEM), 587 (2002) 97.

[19] S. McDonald, L. Ojamäe, L. S.J. Singer, J. Phys. Chem. A, 102 (1998) 2824.

[20] B. Hartke, Phys. Chem. Chem. Phys., 5 (2003) 275.

[21] K. A. Udachin, C.I. Ratcliffe, G.D. Enright, J. A. Ripmeester, Supramolecular Chemistry, 8 (1997) 173.

[22] B. L. Zhang, C. Z. Wang, K. M. Ho, C. H. Xu, C. T. Chan, J. Chem. Phys., 97 (1992) 5007.

[23] J.-L. Kuo, J.V. Coe, S.J. Singer, Y.B. Band, L. Ojamäe, J. Chem. Phys., 114 (2001) 2527.

[24] D. Eisenberg, W. Kauzmann, The Structure and Properties of Water, Oxford University Press, Oxford, 1969.

[25] C. J. Burnham, S. S. Xantheas, J. Mol. Liq., 110 (2004) 177.

[26] E. Whalley, J. Chem. Phys., 81 (1984) 4087.

[27] S.-W. Lee, P. Freivogel, T. Schindler, J.L. Beauchamp, J. Am. Chem. Soc., 120 (1998) 11758.

[28] T. Schindler, C. Berg, G. Niedner-Schattenburg, V.E. Bondybey, Chem. Phys. Lett., 250 (1996) 301.

[29] A. Lenz, L. Ojamäe, J. Chem. Phys., 131 (2009) 134302.

**Table 1** Properties for the small clusters with 15-34 water molecules. *N*2, *N*3, *N*4 and *N*5 denote the number of 2-, 3-, 4- and 5-coordinated molecules, and "H-bonds" denotes the average numbers of H-bonds per water molecule. B3LYP and MP2 electronic interaction energies, $\Delta E$, and B3LYP Gibbs free energies at 298 K, $\Delta G$, are given in kJ (mol $H_2O$)$^{-1}$.

| cluster | cage-based structures [4,17] | | | | | | | TTM2-F global minimum structures [9] | | | | | | | |
|---|---|---|---|---|---|---|---|---|---|---|---|---|---|---|---|
| size | *N*2 | *N*3 | *N*4 | H-bonds | $\Delta E_{B3LYP}$ | $\Delta E_{MP2}$ | $\Delta G_{B3LYP}$ | *N*2 | *N*3 | *N*4 | *N*5 | H-bonds | $\Delta E_{B3LYP}$ | $\Delta E_{MP2}$ | $\Delta G_{B3LYP}$ |
| 15 | 1 | 14 | – | 2.93 | -45.6 | -47.5 | 2.2 | – | 10 | 5 | – | 3.33 | -46.3 | -49.1 | 2.9 |
| 16 | – | 16 | – | 3.00 | -46.6 | -48.4 | 1.7 | – | 8 | 8 | – | 3.50 | -46.4 | -49.3 | 3.4 |
| 17 | 1 | 16 | – | 2.94 | -45.1 | -48.1 | 3.0 | – | 12 | 5 | – | 3.29 | -46.7 | -50.0 | 3.0 |
| 18 | – | 18 | – | 3.00 | -46.5 | -48.3 | 2.4 | – | 10 | 8 | – | 3.44 | -47.3 | -50.2 | 2.8 |
| 19 | – | 18 | 1 | 3.05 | -46.5 | -48.6 | 2.4 | – | 14 | 3 | 2 | 3.36 | -47.5 | -50.9 | 2.8 |
| 20 | – | 20 | – | 3.00 | -47.2 | -49.2 | 2.1 | – | 12 | 8 | – | 3.40 | -48.3 | -51.3 | 2.2 |
| 21[a] | – | 16 | 5 | 3.24 | -48.3 | -51.6 | 1.8 | – | 16 | 5 | – | 3.24 | -48.5 | -51.2 | 1.9 |
| 22 | 1 | 16 | 5 | 3.18 | -47.5 | -50.0 | 2.6 | – | 12 | 10 | – | 3.45 | -47.8 | -51.3 | 2.8 |
| 23 | – | – | – | – | – | – | – | – | 14 | 9 | – | 3.39 | -48.4 | -52.0 | 2.5 |
| 24 | – | – | – | – | – | – | – | – | 12 | 12 | – | 3.50 | -49.0 | -52.2 | 2.3 |
| 25 | – | – | – | – | – | – | – | – | 16 | 9 | – | 3.36 | -49.5 | -52.8 | 1.5 |
| 26 | – | – | – | – | – | – | – | – | 17 | 8 | 1 | 3.38 | -49.6 | -52.9 | 1.6 |
| 27 | – | – | – | – | – | – | – | – | 18 | 9 | – | 3.33 | -50.0 | -53.2 | 1.3 |
| 28 | – | 20 | 8 | 3.29 | -48.8 | -52.4 | 2.1 | 1 | 15 | 11 | 1 | 3.43 | -48.7 | -52.9 | 2.5 |
| 29 | – | – | – | – | – | – | – | – | 16 | 13 | – | 3.45 | -50.0 | -53.5 | 1.6 |
| 30 | – | 22 | 8 | 3.27 | -48.1 | -51.5 | 2.5 | – | 14 | 16 | – | 3.53 | -49.0 | -53.5 | 2.8 |
| 31 | – | – | – | – | – | – | – | – | 16 | 15 | – | 3.48 | -49.5 | -53.7 | 2.3 |
| 32 | – | – | – | – | – | – | – | 1 | 14 | 17 | – | 3.50 | -49.5 | -53.5 | 2.1 |
| 33 | – | – | – | – | – | – | – | 1 | 15 | 16 | 1 | 3.52 | -49.3 | -53.5 | 2.4 |
| 34 | – | – | – | – | – | – | – | – | 16 | 18 | – | 3.53 | -49.6 | -54.0 | 2.4 |

a: The cage-based and TTM2-F entries for the 21 molecule cluster correspond to the same oxygen framework but with slightly different H-bond topologies.

**Table 2** Properties for the large clusters. *N*3 and *N*4 denote the number of 3- and 4-coordinated molecules. The average numbers of H-bonds per water molecule are given. B3LYP and MP2 electronic interaction energies, $\Delta E$, and Gibbs free energies at 298 K, $\Delta G$, are given in kJ (mol $H_2O$)$^{-1}$.

| size | type | *N*3 | *N*4 | H-bonds | $\Delta E_{B3LYP}$ | $\Delta E_{MP2}$ | $\Delta G_{B3LYP}$ |
|---|---|---|---|---|---|---|---|
| 35 | 5-ring in 30 cage | 20 | 15 | 3.43 | -48.50 | -52.3 | 3.25 |
| 42 | 6-ring in 36 cage ($S_6$ symmetry) | 24 | 18 | 3.43 | -51.19 | -55.0 | 0.97 |
| 54 | 6-ring in 48 cage | 36 | 18 | 3.33 | -50.16 | -53.6 | 2.19 |
| 55 | 6-ring +1 in 48 cage | 36 | 19 | 3.35 | -50.00 | -53.7 | 2.22 |
| 80 | 20 in 60 cage | 40 | 40 | 3.50 | -51.78 | -56.1 | 1.59 |
| 81 | 21 in 60 cage | 44 | 37 | 3.46 | -50.81 | -55.6 | 2.44 |
| 100 | 20 in 80 cage ($C_{2h}$ symmetry) | 60 | 40 | 3.40 | -53.96 | -57.3 | -0.30 |

**Fig. 1** (Color online) The $(H_2O)_{100}$ cluster where the oxygen framework is taken from crystallographic data [1]. The oxygens of the water molecules in the central dodecahedral are colored blue and the oxygens of the molecules H-bonding to the dodecahedral and the surrounding 5-membered rings are colored green.

**Fig. 2** (Color online) Geometries for the cage-shaped clusters, $(H_2O)_n$, n=15-22, 28 and 30.

**Fig. 3** (Color online) B3LYP/6-31+G(d,p) optimized geometries for the denser clusters, originally obtained in Ref. [9] by an evolutionary algorithm and TTM2-F [9].

**Fig. 4** (Color online) Geometries for the clusters, $(H_2O)_n$, n = 35, 42, 54, 55, 80 and 81. The oxygens of the water molecules inside the cage are colored blue and the oxygens of the molecules in the cage that are bonded to the inserted molecules green.

**Fig. 5** B3LYP/6-31+G(d,p) (circles) and MP2/6-31+G(d,p) (triangles) interaction energies for the cage-shaped clusters (filled) and the denser structures [9] (open). The solid line shows the fitted curves, $\Delta E_{B3LYP} = -54.5 + 13.4(n - 11.1)^{-1/3}$ and $\Delta E_{MP2} = -65.4 + 34.6(n - 5.6)^{-1/3}$.

**Fig. 6** Energy differences between the cage-based clusters and the denser clusters [9], using MP2 (triangles) and B3LYP (circles). Electronic energies (solid line), electronic energies scaled to agree with the experimental energy for the dimer (dotted line) and Gibbs free energies based on scaled electronic energies (B3LYP or MP2) and B3LYP free energy corrections (dashed line). A negative value implies the cage-based structures to be more stable.

**Fig. 7** Gibbs free energy for the cage-shaped clusters (filled triangles) and the denser structures [9] (open triangles).

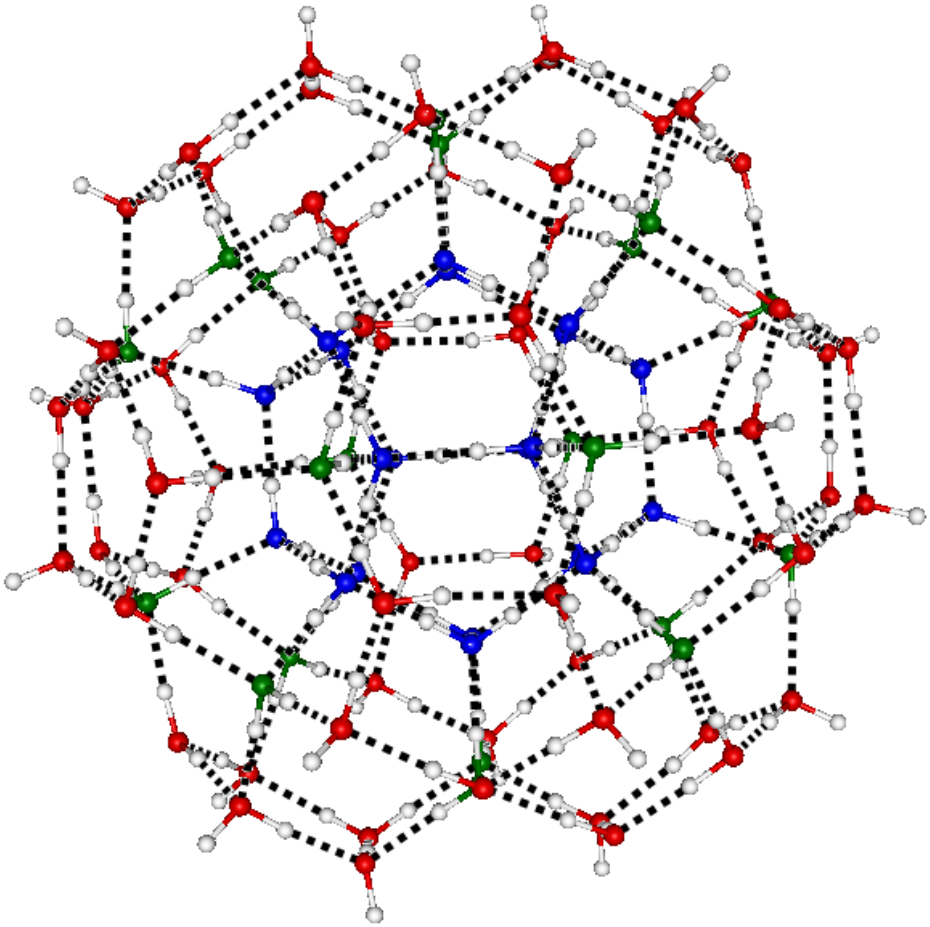

Fig. 1. A. Lenz and L. Ojamäe,

*Computational studies of the stability of the* $(H_2O)_{100}$ *nanodrop*

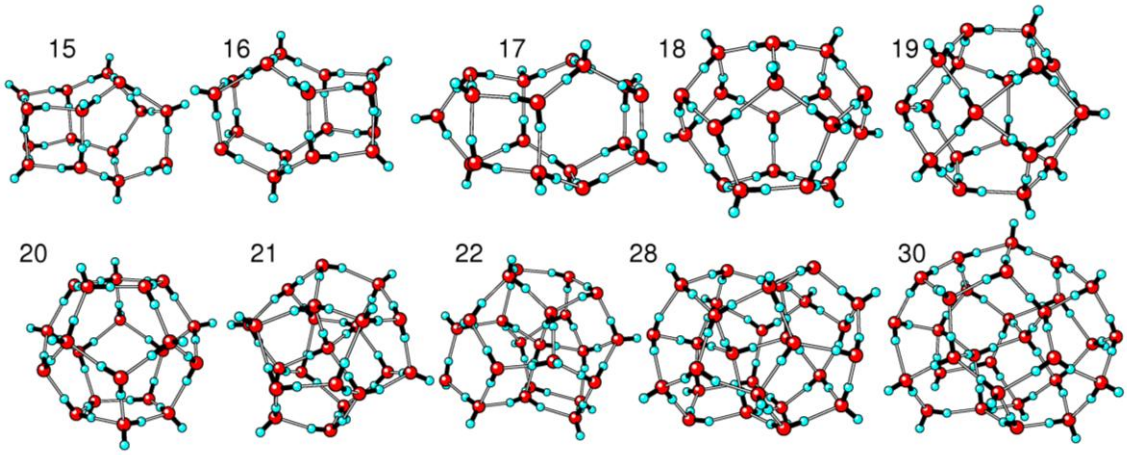


Fig. 2. A. Lenz and L. Ojamäe,

*Computational studies of the stability of the* $(H_2O)_{100}$ *nanodrop*

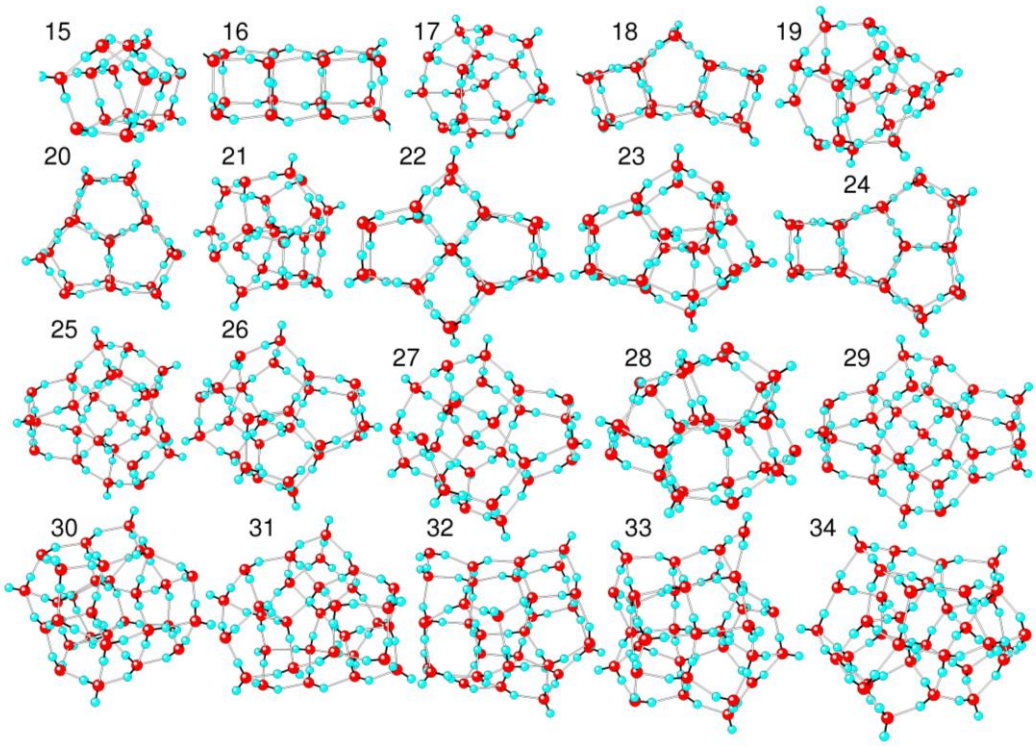


Fig. 3. A. Lenz and L. Ojamäe,

*Computational studies of the stability of the $(H_2O)_{100}$ nanodrop*

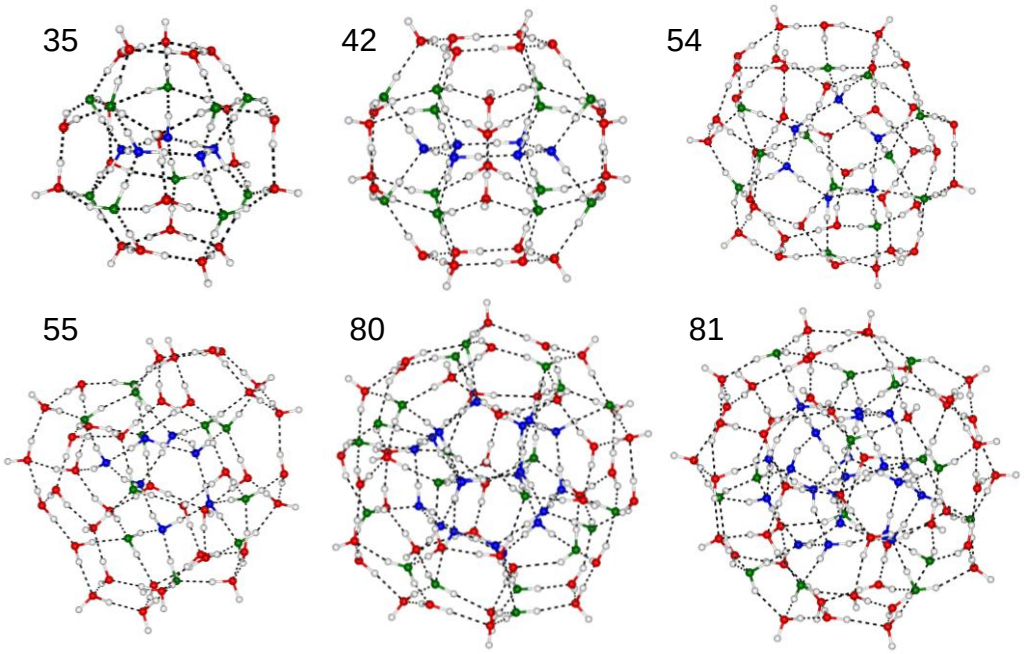


Fig. 4. A. Lenz and L. Ojamäe,

*Computational studies of the stability of the $(H_2O)_{100}$ nanodrop*

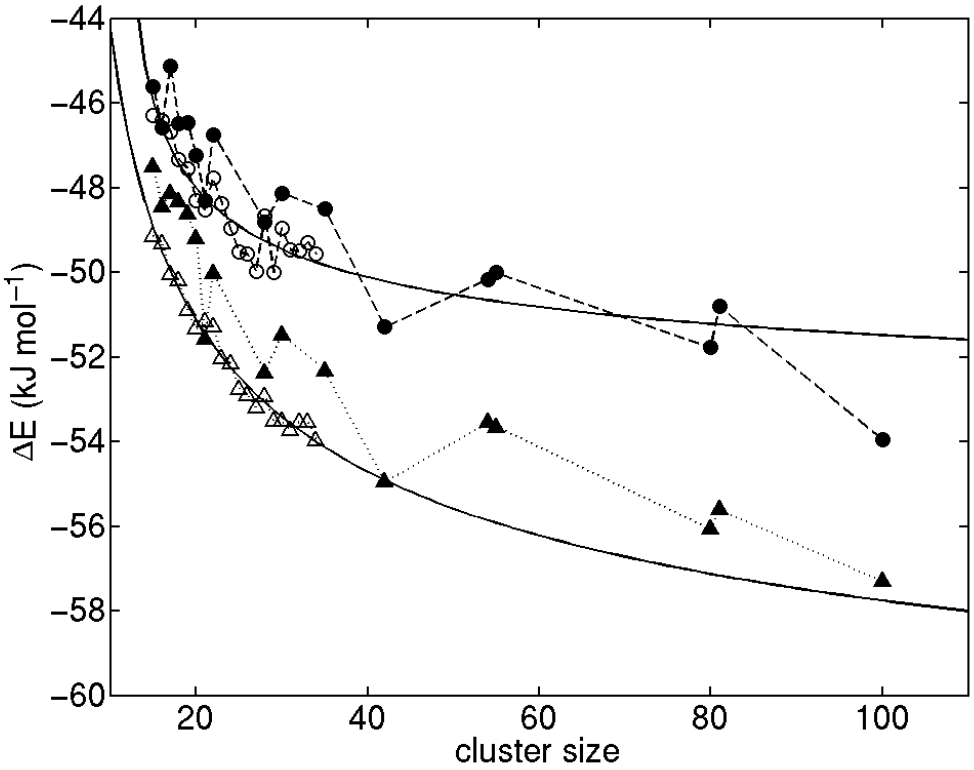


Fig. 5. A. Lenz and L. Ojamäe,

*Computational studies of the stability of the $(H_2O)_{100}$ nanodrop*

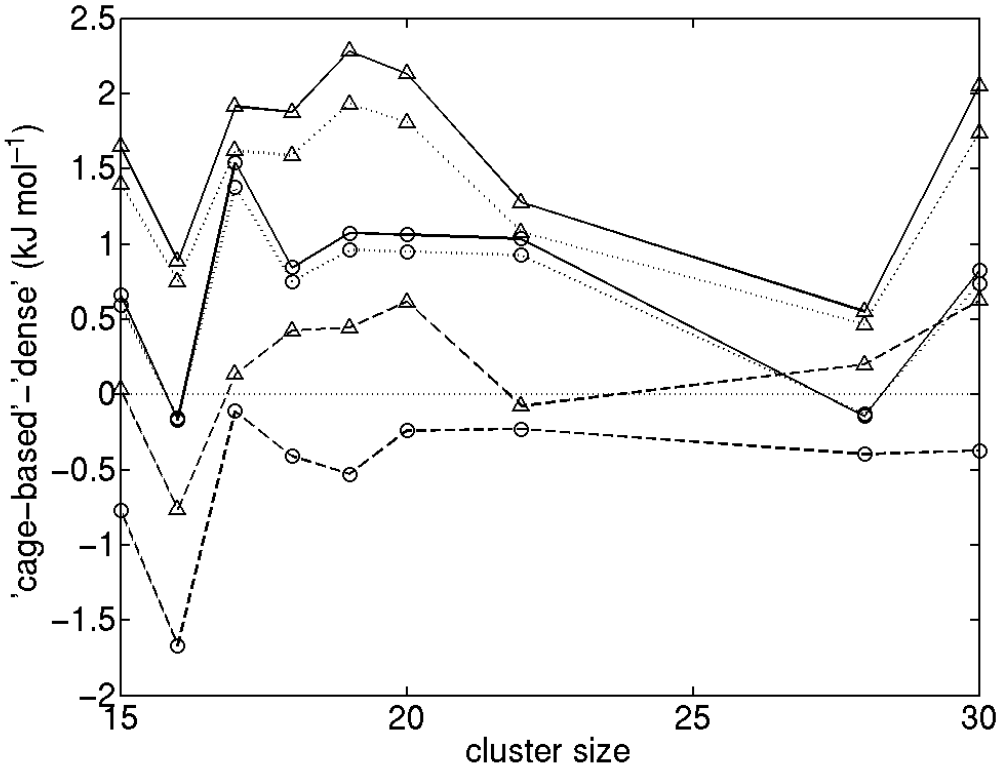


Fig. 6. A. Lenz and L. Ojamäe,

*Computational studies of the stability of the* $(H_2O)_{100}$ *nanodrop*

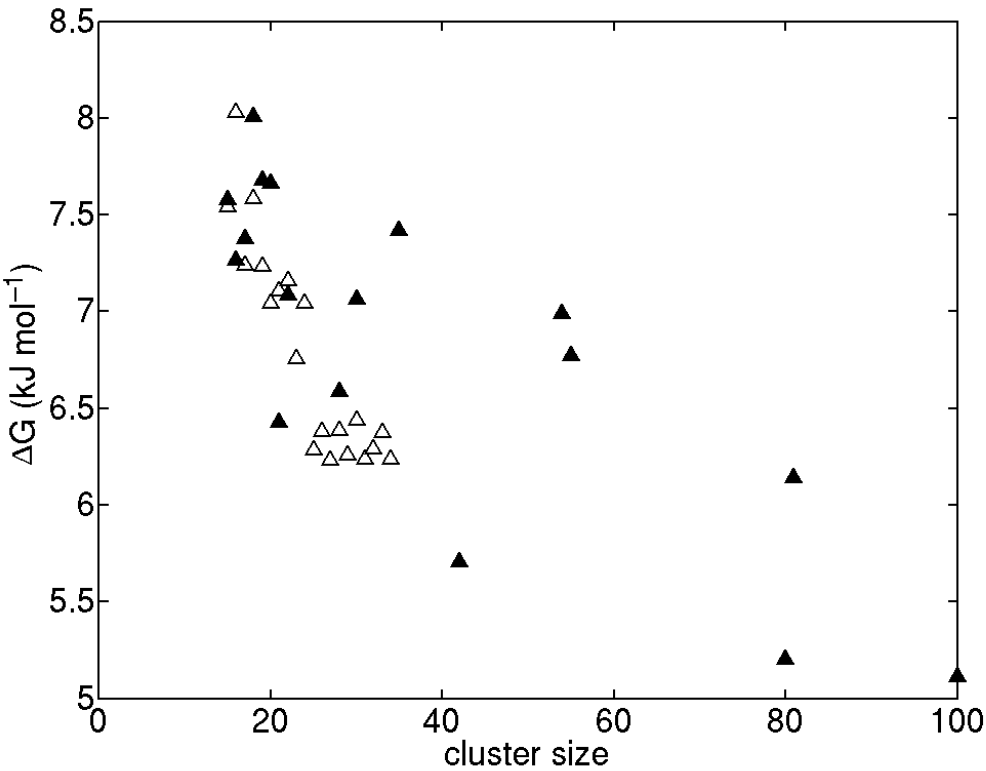


Fig. 7. A. Lenz and L. Ojamäe,

*Computational studies of the stability of the* $(H_2O)_{100}$ *nanodrop*